13th World Conference on Earthquake Engineering
Vancouver, B.C., Canada
August 1-6, 2004
Paper No. 2376

EXPLICIT CONSTITUTIVE RELATIONSHIP FOR AXIALLY LOADED CONCRETE CONFINED BY FRP

Tommaso ALBANESI[1], Camillo NUTI[2], Ivo VANZI[3]

SUMMARY

Fiber-reinforced polymer (FRP) tubes filled with concrete are very effective structural elements when loaded under axial stress. The exterior jacket of FRP, in fact, confines the inner concrete and significantly enhances both its resistance and stiffness. On the other hand FRP protects the inner core from temperature and humidity effects, and may also be used both as formwork and as reinforcement. Nonetheless, stability problems arise when FRP tubes are used as slender structural elements. Although the physical behavior of a straight structural element is simple, state-of-the-art models on one side do not deal explicitly with instability effects, on the other do not offer closed form solutions for the longitudinal constitutive relationship. The former aspect is dealt with in Albanesi [1]. In this paper, first a closed form constitutive relationship for concrete filled FRP squat tubes is developed and validated against experimental results and other state-of-the-art models. Secondly, design charts for FRP squat tubes under compression are obtained as a function of the most important variables and used to verify example elements. The proposed model shows a good capability of describing the behavior of FRP-concrete tubes, while being simple to use, expressed in a closed form and hence computationally fast.

INTRODUCTION

Jacketing is an old technique widely used to improve the mechanical properties of structural members. Traditionally, the technique is applied to beam and column elements to increase resistance and stiffness in shear and bending, using external elements like jackets or plates made of steel or reinforced concrete.

More recently, after the adoption of FRP among the civil engineering materials, researchers have focused their attention on more innovative applications. Some peculiar properties of FRP's, resistance to corrosion, lightness, ease of use in difficult yards, have made a wide range of applications on new and existing structures successful. Such applications include reservoirs, foundations and port piles, for new constructions, and wrapping of beams and columns for existing ones.

In this work the simplest FRP – concrete structural element is studied: an annular FRP tube, filled with concrete and loaded in compression. Notwithstanding the simplicity of the physical problem, existing models are either accurate but complex or of simple use but inaccurate in some range of the constitutive relationships.

Let us first discuss the physical behavior of a wrapped concrete specimen under compression and then briefly review state-of-the-art models. When the concrete core is loaded in compression, it

[1] Assistant Professor of Structural Engineering, Dip. di Progettazione, Riabilitazione e Controllo delle Strutture, University “G. D'Annunzio” of Chieti, Pescara, Italy, e-mail: t.albanesi@pricos.unich.it
[2] Full Professor of Structural Engineering, Dipartimento di Strutture, University of Roma Tre, Rome, Italy, e-mail: c.nuti@uniroma3.it
[3] Associate Professor of Structural Engineering, Dip. di Progettazione, Riabilitazione e Controllo delle Strutture, University G. D'Annunzio of Chieti, Pescara, Italy, e-mail: i.vanzi@pricos.unich.it

dilates according to the (non linear) Poisson ratio [2]. This expansion is contrasted by the tube which applies a hydrostatic – like pressure to the core and hence improves its stiffness and resistance. This clearly recognized aspect in reinforced concrete motivates the requirements for steel stirrups which is present in all the Codes. However the beneficial effect of confinement requires the concrete to have gone a *sufficiently* large lateral expansion to develop; for instance FRP wrapping starts to be effective only at a stress equal to about 60-70% times the unconfined concrete failure stress.
FRP also is longitudinally stressed, either because it is directly loaded or because of stress transfer from concrete to FRP due to bond; this fact is generally not fully recognized although it can have important and undesired consequences. In fact, longitudinal loading of FRP causes it to expand laterally and hence to give a lesser degree of confinement. If a steel tube is used instead of FRP, this is the main reason why it is effective only after concrete has been considerably damaged [3]: in the elastic range in fact, the Poisson ratio of steel (about 0.30) is considerably higher than that of concrete (about 0.10–0.15) and so the steel jacket is, at best, ineffective at the start. For FRP the problem is less important because of two reasons: firstly, its Poisson ratio is lower than that of steel, ranging from 0.015 for carbon FRP (CFRP) to 0.06 for glass FRP (GFRP) [4]; these values are the expansion perpendicular to the loading direction, which is assumed coincident with the direction of minimum stiffness. Secondly, the mechanical properties of FRP can be designed independently along the two main directions and hence a material which is very flexible in the longitudinal direction and hence little loaded, can be put in place. If the above is recognized and taken care for, one can design and put in place an FRP jacket which minimizes the dependence between longitudinal and transverse behavior, making it negligible; this assumption (made in this work) allows to focus the attention only on the FRP behavior in the transverse direction. A further important aspect is that FRP is prevented from buckling by the presence of the concrete inner core.
Thus, the FRP tube and the concrete core interact in a mutually beneficial way, the former confining the latter and the latter avoiding buckling of the former; the result is that the concrete characteristics are strongly enhanced.
State-of-the-art models can be grouped in two broad categories, which can be termed *physically* and *experimentally* based models. An extensive recent review of strength models con be found in Lam [5] and Teng [6].
The first class contains models (e.g. Spoelstra [7], Fam [8]) which develop the wrapped concrete constitutive law using equilibrium and compatibility conditions departing from known simpler models for concrete confined by a constant hydrostatic – like pressure.
Spoelstra and Monti used the formulation of Pantazopolou [9] while Fam and Rizkalla the one proposed by Mander [10]. Since FRP exerts a continuously varying confining pressure on concrete, which is not explicitly accounted for neither in the Pantazopolu and Mills nor in the Mander formulations, both solution schemes use an iterative procedure to compute the longitudinal σ–ε law: given a value of longitudinal deformation, the problem in the transverse cross-section is solved with a trial and error procedure using transverse equilibrium and compatibility relationships. Both approaches are accurate and capable of catching also the details of the constitutive relationship but the solution schemes are neither direct nor simple to implement.
To the second class belong instead models which are based on experimental results. They are simple to understand and implement but less accurate and incapable of catching the details of the confined concrete behavior. A well – known and nicely working model was proposed by Samaan [11]. They pragmatically recognize that the constitutive law of confined concrete is almost entirely explained by assuming that, at the beginning, the resisting mechanism is concrete only and that, after concrete has sufficiently dilated, the FRP jacket starts to be effective and the behavior depends on the FRP – concrete interaction. Therefore the full constitutive law is composed of two straight segments, in which the first one is coincident with the one for unconfined concrete and the second one accounts for the interaction, and a monotonic curve connecting them. The weak point of this model is in the range connecting the two segments: depending on the problem at hand, the experimental behavior can be widely different varying from a smooth and monotonous transition to an uneven one, containing intervals with zero or negative stiffnesses.
The model proposed in this paper belongs to the class of *physical* procedures; departing from the Mander model for confined concrete, the problem of solving for compatibility and equilibrium in the transverse direction is faced and solved. The main difference with respect to the other mentioned

physical procedures is that, by doing some opportune simplifications, the transverse problem can be solved in a straightforward way so that a constitutive model can be expressed in closed form avoiding trial and error procedures. This is not a trivial aspect because the simplicity of the final formulation allows: (i) the variables governing the problem to be easily identified and presented in charts (ii) doing parametric studies to assess their influence (iii) the tangent stiffness of confined concrete and the buckling load for a confined concrete column to be computed in closed form (Albanesi [1]).
The presented model has been tested using many experimental results and compared with state-of-the-art models. The selected cases are squat tubes which fail in compression. Comparisons between experiments and model predictions are, as it will be shown, satisfying.

CONSTITUTIVE MODEL FOR SQUAT FRP – CONCRETE TUBES

Longitudinal behavior of confined concrete

The problem of circular FRP confined concrete sections under compression is axial symmetric. A flexible and accurate model for concrete under constant confinement pressure σ_r was presented by Mander [10] based on a wide range of experimental tests.
The longitudinal stress f_{cc} which causes the confined concrete to deform by ε_{cc} is computed as:

$$\frac{f_{cc}}{f'_{cc}} = \frac{xr}{r-1+x^r}\ ; \quad x = \frac{\varepsilon_{cc}}{\varepsilon'_{cc}}\ ; \quad r = \frac{E_{co}}{E_{co}-E_{ccs}} \tag{1}$$

where f'_{cc} is the confined concrete strength, ε'_{cc} is the strain at maximum strength f'_{cc}, E_{co} is the initial tangent elastic modulus of unconfined concrete and $E_{ccs}=f'_{cc}/\varepsilon'_{cc}$ is the secant modulus of confined concrete at maximum strength.
The value of the initial tangent elastic modulus of concrete may be correlated to its unconfined axial strength, f'_{co}, through a constant α (which may vary from 4000 to 5700): $E_{co} = \alpha\sqrt{f'_{co}}$ (MPa).
The confined concrete strength f'_{cc} can be correlated with its unconfined axial strength f'_{co} via a nonlinear function of the normalized confining pressure σ_r/f'_{co} as follows:

$$\frac{f'_{cc}}{f'_{co}} = 2.254\sqrt{1+7.940\frac{\sigma_r}{f'_{co}}} \text{-} 2\frac{\sigma_r}{f'_{co}} \text{-} 1.254 \tag{2}$$

With f'_{cc} known, the strain at maximum strength ε'_{cc} can be computed as:

$$\frac{\varepsilon'_{cc}}{\varepsilon'_{co}} = 1+5\left(\frac{f'_{cc}}{f'_{co}}-1\right) = 5\frac{f'_{cc}}{f'_{co}}-4 \tag{3}$$

where ε'_{co} is the strain at peak strength of unconfined concrete.
Notice that Eq. (3) is a linear function of strengthening ratio f'_{cc}/f'_{co} and thus has the same functional dependence on the confinement ratio as Eq. (2).
Through Eqs. (2) and (3), the secant modulus of confined concrete E_{ccs} is then computed as the secant modulus of unconfined concrete at maximum strength $E_{cs}=f'_{co}/\varepsilon'_{co}$ times the ratio of two nonlinear functions of the normalized confining pressure.

Transverse behavior of confined concrete

A simple and accurate model to describe transverse deformation in terms of the longitudinal one has been recently presented by Fam [8]. Departing from the experimental results of Gardner [12], who tested concrete cylinders under constant hydrostatic-like pressure, they proposed the following relationship between the Poisson ratios of unconfined (ν_{co}) and confined (ν_{cc}) concrete:

$$\frac{\nu_{cc}}{\nu_{co}} = \left(1.914\frac{\sigma_r}{f'_{co}} + 0.719\right)\frac{\varepsilon_{cc}}{\varepsilon'_{cc}} + 1 \tag{4}$$

The above equation allows the transverse strain in concrete ε_l to be expressed as a function of the longitudinal one ε_{cc} of the strain at peak strength ε'_{cc} of the confinement ratio and of the initial Poisson ratio of unconfined concrete ν_{co} as:

$$\varepsilon_l = \nu_{cc}\varepsilon_{cc} \tag{5}$$

Transverse behavior of the FRP jacket

Compatibility of FRP and concrete displacements requires equality of the transverse deformations of concrete ε_l and jacket ε_j (ε_l=ε_j). This means that the radial pressure on concrete σ_r can be expressed as:

$$\sigma_r = \frac{\sigma_j t}{R} = \frac{E_{jho} t}{R}\varepsilon_l \tag{6}$$

where σ_j and E_{jho} are the stress and elastic modulus of tube in hoop direction and t and R are the thickness and the radius of confining tube, respectively.

Hence the normalized confining pressure can be written as:

$$\bar{\sigma}_r = \frac{\sigma_r}{f'_{co}} = k_{fc} \cdot \frac{\varepsilon_l}{\varepsilon'_{co}} \tag{7}$$

$$k_{fc} = \frac{E_{jho}}{E_{cs}} \cdot \frac{t}{R} \tag{8}$$

The confinement stiffness ratio of FRP-concrete tube, k_{fc}, has been explicitly highlighted because, as it will be shown in the next sections, it is the only parameter needed to describe the longitudinal constitutive relationship of confined concrete. Notice that k_{fc} may vary between 0 and about 0.17; the latter value has been obtained considering carbon composites (E_{jho}≅210 GPa), concrete with E_{cs}=12.5 GPa, and t/R=0.01. In the parametric studies that follow, for the sake of completeness, the maximum for k_{fc} has been considered equal to 2.

Proposed longitudinal constitutive relationship of confined concrete

Through Eq. (7), Eq. (2) can be rewritten as:

$$\frac{f'_{cc}}{f'_{co}} = 2.254\sqrt{1+7.94\bar{\sigma}_r} - 2\bar{\sigma}_r - 1.254 \tag{9}$$

Expression (9) is a non linear function of the lateral response strain, ε_l, because of the presence of the term within the square root:

$$y(\bar{\sigma}_r) = \sqrt{1+7.94\bar{\sigma}_r} \tag{10}$$

The latter can be however reasonably well approximated with a linear function as follows:

$$y_{appr}(\bar{\sigma}_r) = 1 + C_1 \cdot \bar{\sigma}_r \tag{11}$$

where the constant C_1 can be computed by setting to zero the value of $\Delta(C_1)$:

$$\Delta(C_1)=\int_0^{\bar{\sigma}_{max}}\left[y(\bar{\sigma}_r)-y_{appr}(\bar{\sigma}_r)\right]^3\cdot d\bar{\sigma}_r \tag{12}$$

The value of $\bar{\sigma}_{r\max}$ can be determined by noting that:

$$\bar{\sigma}_{r\max}=\frac{(\sigma_j)_{\max}}{(f'_{co})_{\min}}\cdot\left[\frac{t}{R}\right]_{\max} \tag{13}$$

Assuming, for commercial FRP's $(\sigma_j)_{max}$=1750 MPa (Matthews [4], Hollaway [13]), $(f'_{co})_{min}$=25 MPa and $(t/R)_{max}$=0.01, Eq. (13) yields $\bar{\sigma}_{r\max}$=0.70.
Thus, accepting the limitations on $\bar{\sigma}_{r\max}$ and the error of about 7% in approximating $y(\bar{\sigma}_r)$, it can be assumed C_1=2.488.
Equations (9) and (3) can be written respectively as:

$$\frac{f'_{cc}}{f'_{co}}\cong 1+3.609\cdot\bar{\sigma}_r \tag{14}$$

$$\frac{\varepsilon'_{cc}}{\varepsilon'_{co}}\cong 1+18.045\cdot\bar{\sigma}_r \tag{15}$$

The two above equations are linear functions of ε_l . Substituting equations (7) and (15) into equation (4) gives:

$$\frac{\nu_{cc}}{\nu_{co}}\cong\frac{0.719+1.914\cdot\bar{\sigma}_r}{1+18.045\cdot\bar{\sigma}_r}\frac{\varepsilon_{cc}}{\varepsilon'_{co}}+1 \tag{16}$$

Equations (5) and (16) constitute a system of two independent equations in the three unknowns ν_{cc}, ε_{cc} and ε_l. The system can be solved for ε_l for a given value of ε_{cc}. Substituting Eq. (16) in Eq. (5) the following expression is obtained:

$$\frac{N}{D}=0 \tag{17}$$

in which:

$$N=10.159k_{f_c}\frac{\varepsilon_l^2}{\varepsilon_{co}'^2}+\left[0.563-10.159k_{f_c}\nu_{co}\frac{\varepsilon_{cc}}{\varepsilon'_{co}}-1.077k_{f_c}\nu_{co}\frac{\varepsilon_{cc}^2}{\varepsilon_{co}'^2}\right]\frac{\varepsilon_l}{\varepsilon'_{co}}-\left(0.563+0.405\frac{\varepsilon_{cc}}{\varepsilon'_{co}}\right)\nu_{co}\frac{\varepsilon_{cc}}{\varepsilon'_{co}} \tag{18}$$

$$D=10.159k_{f_c}\frac{\varepsilon_l}{\varepsilon'_{co}}+0.563 \tag{19}$$

Observing $D\neq 0$ (since $\varepsilon_l\geq 0$ and $0\leq k_{fc}<\infty$), Eq. (17) reduces to $N=0$ which is a parabolic equation in ε_l:

$$a\left(\frac{\varepsilon_l}{\varepsilon'_{co}}\right)^2+b\frac{\varepsilon_l}{\varepsilon'_{co}}+c=0 \tag{20}$$

$$
\begin{aligned}
a &= 10.159 k_{f_c} \\
b &= 0.563 - 10.159 k_{f_c} \nu_{co} \frac{\varepsilon_{cc}}{\varepsilon'_{co}} - 1.077 k_{f_c} \nu_{co} \frac{\varepsilon_{cc}^2}{\varepsilon'^2_{co}} \\
c &= -\left(0.563 + 0.405 \frac{\varepsilon_{cc}}{\varepsilon'_{co}}\right) \nu_{co} \frac{\varepsilon_{cc}}{\varepsilon'_{co}}
\end{aligned}
\tag{21}
$$

The only root with a physical meaning is:

$$
\frac{\varepsilon_l}{\varepsilon'_{co}} = \frac{-b + \sqrt{b^2 - 4 \cdot a \cdot c}}{2 \cdot a} \tag{22}
$$

Notice that, once $\varepsilon_l(k_{fc}, \nu_{co}, \varepsilon_{cc}/\varepsilon'_{co})$ is known, Eqs. (14), (15) and (16) allow the straightforward determination of f'_{cc}, ε'_{cc} and ν_{cc}.

It is now possible to plot all the quantities of interest as a function of $\varepsilon_{cc}/\varepsilon'_{co}$ and k_{fc}, and of the mechanical properties of unconfined concrete (ν_{co}, ε'_{co}, f'_{co}, α). In Figure 1, the plots of $\varepsilon_l(k_{fc}, \nu_{co}, \varepsilon_{cc}/\varepsilon'_{co})/\varepsilon'_{co}$ and $f_{cc}(k_{fc}, \nu_{co}, \varepsilon'_{co}, f'_{co}, \alpha, \varepsilon_{cc}/\varepsilon'_{co})/f'_{co}$ are shown, for fixed values of ν_{co}, ε'_{co}, f'_{co} and α. The plots are obtained using Eqs. (21) and (22) for the former and Eqs. (1), (14), (15), (21) and (22) for the latter.

The branches in Figure 1 are drawn for $0 \le \varepsilon_{cc}/\varepsilon'_{co} \le 25$. It is clear that if the FRP-concrete tube is subjected to increasing longitudinal deformation up to the jacket collapse, there is a global failure. In Figure 1(a) the critical deformation for some commercial FRP's are shown (4Matthews 1996).

Figure 1 show the influence of the stiffness ratio k_{fc} on the behavior of the confined concrete. For a given design, Figure 1(a) can be used to firstly assess the longitudinal strain ε_{ccu} at rupture of the FRP jacket. Once this is known, Figure 1(b) will show the complete constitutive relationship followed up to ε_{ccu}. From the same figure it can be observed that the concrete behavior improves with increasing values of k_{fc}. A particularly interesting feature is that for values of k_{fc} greater than about 0.020 (for the concrete properties specified in the figures) there is no descending branch up to the jacket rupture and hence no negative stiffness.

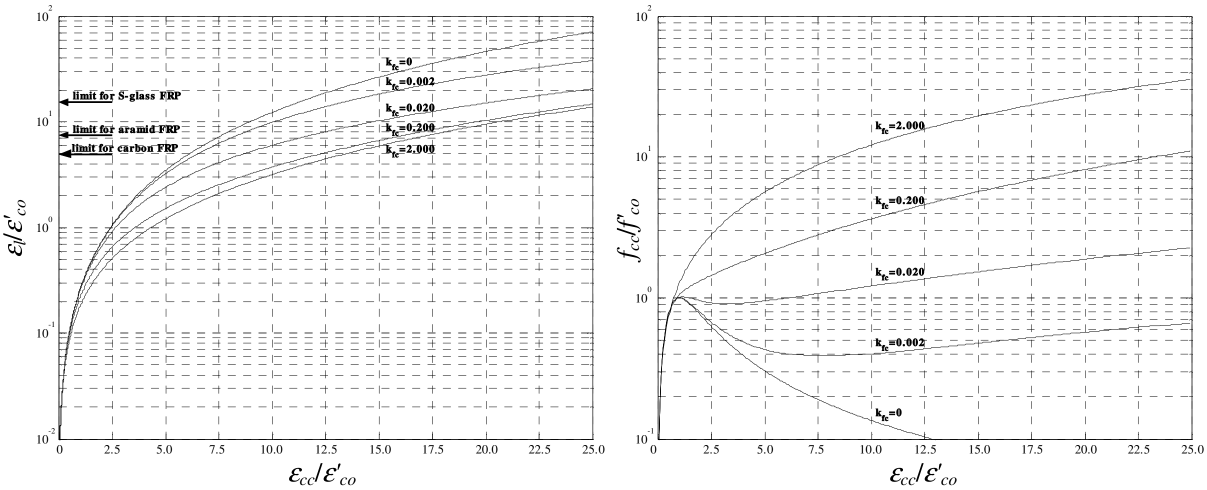

Figure 1. (a) Lateral strain ratio $\varepsilon_l/\varepsilon'_{co}$ and (b) Strengthening ratio f_{cc}/f'_{co} in confined concrete (with ν_{co}=0.15, ε'_{co}=0.002, f'_{co}=30MPa and α=5,000)

This property can be more clearly highlighted evaluating the confined concrete tangent modulus, E_{cc}:

$$
E_{cc} = \frac{df_{cc}}{d\varepsilon_{cc}} \tag{23}
$$

A compact closed form expression for the confined concrete tangent modulus can be found. This can be achieved by formal derivation of f_{cc} (Eq. (1)) with respect to ε_{cc} using the results of the previous section. After considerable algebra, not shown here for the sake of conciseness, E_{cc} has been found to be reasonably simply expressed as:

$$\frac{E_{cc}}{E_{co}}=\left(\frac{f_{cc}}{f'_{cc}}\right)^2\left\{\left(\frac{E_{ccs}}{E_{co}}\right)^2\frac{1-x^r}{x^2}+\left[1+4\cdot\frac{E_{ccs}}{E_{co}}\cdot\frac{\varepsilon'_{co}}{\varepsilon'_{cc}}\cdot\ln\left(x^r\right)\right]\cdot\frac{E_{cs}}{E_{co}}\cdot x^{r-1}\cdot 3.609\cdot k_{f_c}\cdot\frac{d\varepsilon_l}{d\varepsilon_{cc}}\right\} \tag{24}$$

with

$$\frac{d\varepsilon_l}{d\varepsilon_{cc}}=\nu_{co}\left\{\left(0.5+0.106\frac{\varepsilon_{cc}}{\varepsilon'_{co}}\right)+\frac{\left(0.014+0.037\frac{\varepsilon_{cc}}{\varepsilon'_{co}}\right)+\left(0.250+0.079\frac{\varepsilon_{cc}}{\varepsilon'_{co}}+0.006\frac{\varepsilon_{cc}^{\,2}}{\varepsilon'^{\,2}_{co}}\right)\cdot k_{f_c}\cdot\nu_{co}\cdot\frac{\varepsilon_{cc}}{\varepsilon'_{co}}}{\sqrt{\left(0.277+0.090\frac{\varepsilon_{cc}}{\varepsilon'_{co}}+0.003\frac{\varepsilon_{cc}^{\,2}}{\varepsilon'^{\,2}_{co}}\right)k_{f_c}\cdot\nu_{co}\cdot\frac{\varepsilon_{cc}}{\varepsilon'_{co}}}}\right\} \tag{25}$$

Eqs. (24) and (25), although not suited for hand calculation, can be easily programmed with a personal computer.
The above relations are also useful to compute in a closed form the buckling load for an FRP – concrete circular column (see Albanesi [1]).
The variability of $E_{cc}(k_{fc}, \nu_{co}, \varepsilon'_{co}, f'_{co}, \alpha, \varepsilon_{cc}/\varepsilon'_{co})/E_{co}$ with respect to $\varepsilon_{cc}/\varepsilon'_{co}$ is shown in Figure 2(a).
Notice again that for values of k_{fc} greater than 0.020, no negative stiffness exist in the element behavior. Very little difference between the behaviors of specimen with different k_{fc} is observed up to about ε_{cc}=0.70ε'_{co}. In this range, the stiffness decreases almost linearly from the initial value of E_{co} to about 0.70E_{co}. For ε_{cc}>0.70ε'_{co} the tangent stiffness varies widely for different stiffness ratios. For k_{fc}=2.000 it is worth 0.60÷0.90E_{co}; for k_{fc}=0.200 it is worth 0.15÷0.30E_{co}; for lower k_{fc} values it is only a small fraction of E_{co} or it is negative.
In order to clarify the use of the proposed model and highlight the independent and dependent variables, Figure 2(b) shows which equations must be used to compute the longitudinal stress f_{cc} departing from the longitudinal deformation, ε_{cc}. The model for squat tube is shown.
It is worth noticing once again that all the dependent variables are computed in closed form, without having to resort to trial and error procedures.

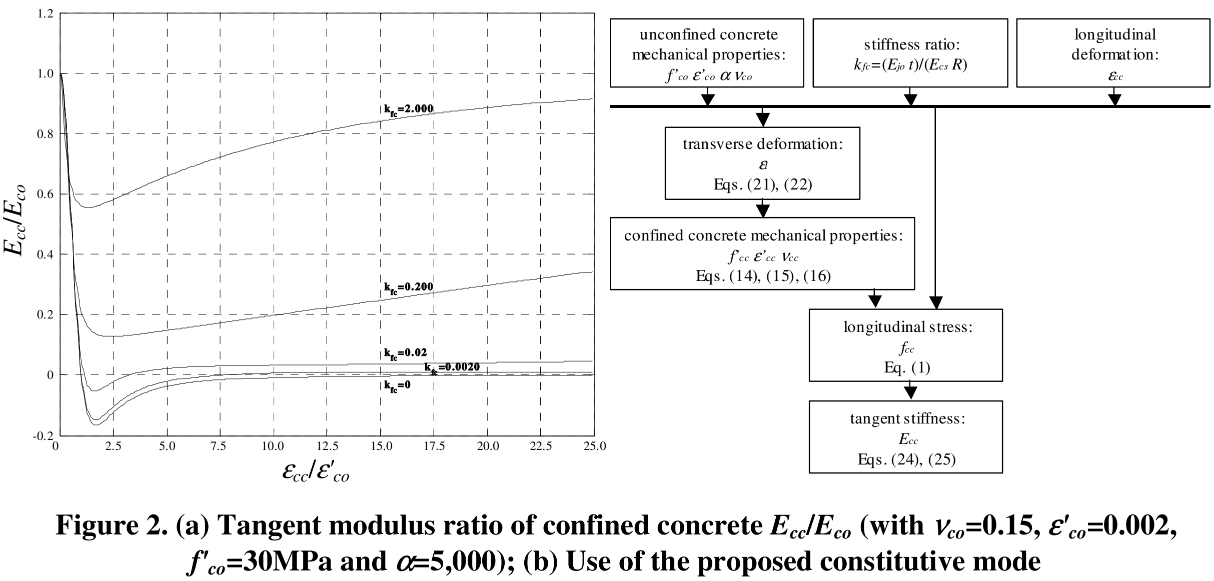

Figure 2. (a) Tangent modulus ratio of confined concrete E_{cc}/E_{co} (with ν_{co}=0.15, ε'_{co}=0.002, f'_{co}=30MPa and α=5,000); (b) Use of the proposed constitutive mode

VALIDATION OF THE MODEL FOR SQUAT TUBES

The *ANV* model has been tested using many experimental results found in literature and has also been compared to other theoretical models.

Table 1. Geometric and mechanical properties of FRP-Confined concrete squat specimens for ANV model validation: (A/L=axial/lateral, n.a.=not available)

Acro-nym	Test reference	Strain resp.	D (mm)	L (mm)	f'_{co} (MPa)	Fiber type	t (mm)	σ_j (MPa)	E_{jho} (MPa)	k_{fc} (%)
FR	Fam [8]	A	219.0	438	58.30	E-Gl.	2.210	548	33400	2.31
KHH.1	Kawashima [15]	A/L	200.0	600	39.00	Carb.	0.338	2810	439000	7.61
KHH.2	Kawashima [15]	A/L	200.0	600	39.00	Carb.	0.676	2327	439000	15.22
M	Mastrapa 1997	A	152.5	305	37.20	S-Gl.	3.070	586	20600	4.46
P.1	Picher [16]	A	152.5	305	39.70	Carb.	3-lay	n.a.	70000	n.a.
P.2	Picher [16]	A	152.5	305	39.70	Carb.	5-lay	n.a.	70000	n.a.
PRL	Picher [17]	A/L	152.0	304	39.70	Carb.	0.900	1245	83000	4.95
SMS.1	Samaan [11]	A	152.5	305	29.64	E-Gl.	1.440	524	37233	4.74
SMS.2	Samaan [11]	A	152.5	305	29.64	E-Gl.	2.200	579	40336	7.85
SMS.3	Samaan [11]	A	152.5	305	29.64	E-Gl.	2.970	641	40749	10.71
SMS.4	Samaan [11]	A	152.5	305	30.86	E-Gl.	1.440	524	37233	4.56

For the sake of brevity, only some of the tests made are presented, those listed in Table 1.
These were selected in order to have a broad range of different situations. The tests include different types of FRP, E-glass, S-glass and carbon, and of concrete ranging from normal (about 30 MPa) to high (about 60 MPa) strength types. Some of the tests have been included also because both axial and lateral responses were recorded. The specimens were different also from a geometrical standpoint: diameter to thickness ratios spaced from a minimum of 50 to a maximum of 600. The confinement stiffness ratio k_{fc} vary from 2.31% to 15.22%. The experimental (dot symbol) axial strain and stress and lateral strain (if available) together with the predictions obtained with *ANV* model (continuous line) and with other models (if available, as listed in Table 2) are shown from Figure 3 to Figure 8.

Table 2. Acronym and reference for the models compared with the proposed one

Acronym	authors and/or reference
ANV	Albanesi, Nuti and Vanzi
AS	Ahmad and Shah 1982 [18]
FK	Fardis and Khalili 1982 [19]
FR	Fam and Rizkalla 2001 [8]
KHH	Kawashima, Hosotani and Hoshikuma 1997 [15]
MPP	Mander, Priestley and Park 1988 [10]
PRL	Picher, Rochette and Labossiere 1996 [17]
SM	Spoelstra and Monti 1999 [7]
SMS	Samaan, Mirmiran and Shahawy 1998 [11]

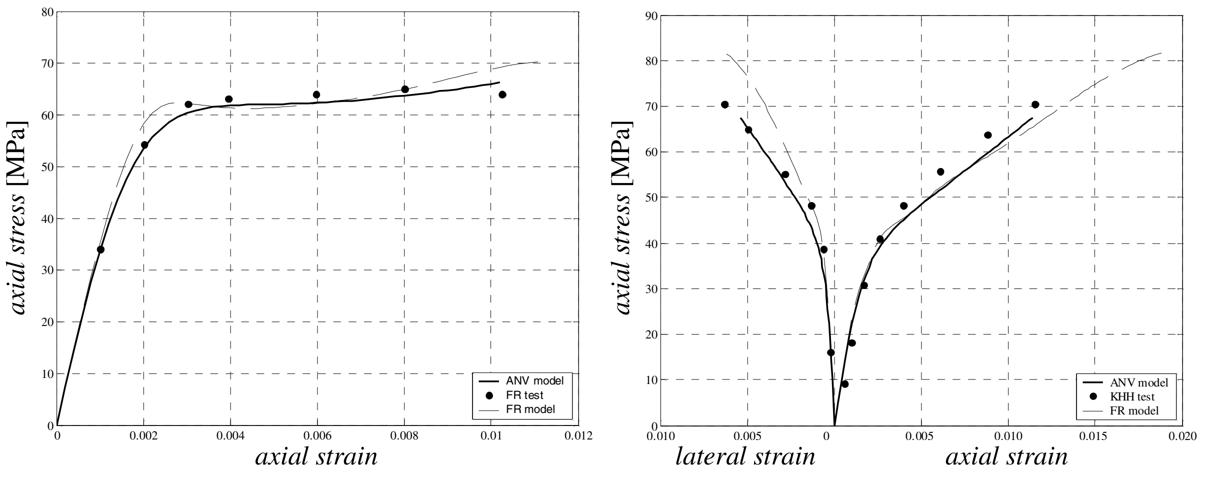

Figure 3. (a) *FR* test vs. *FR* and *ANV* models; (b) *KHH.1* test vs. *FR* and *ANV* models

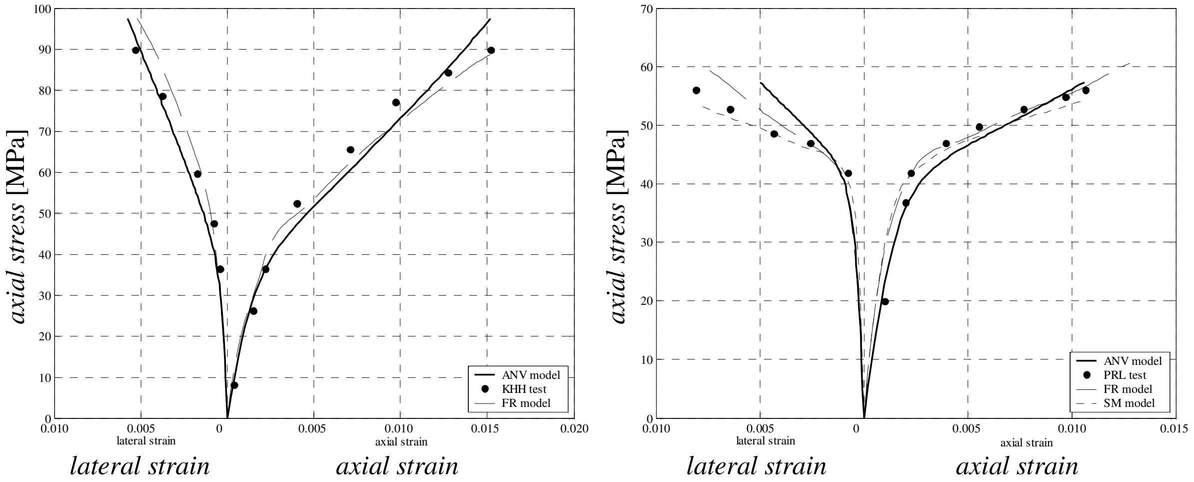

Figure 4. (a) *KHH.2* test vs. *FR* and *ANV* models; (b) *M* test vs. *SMS* and *ANV* models

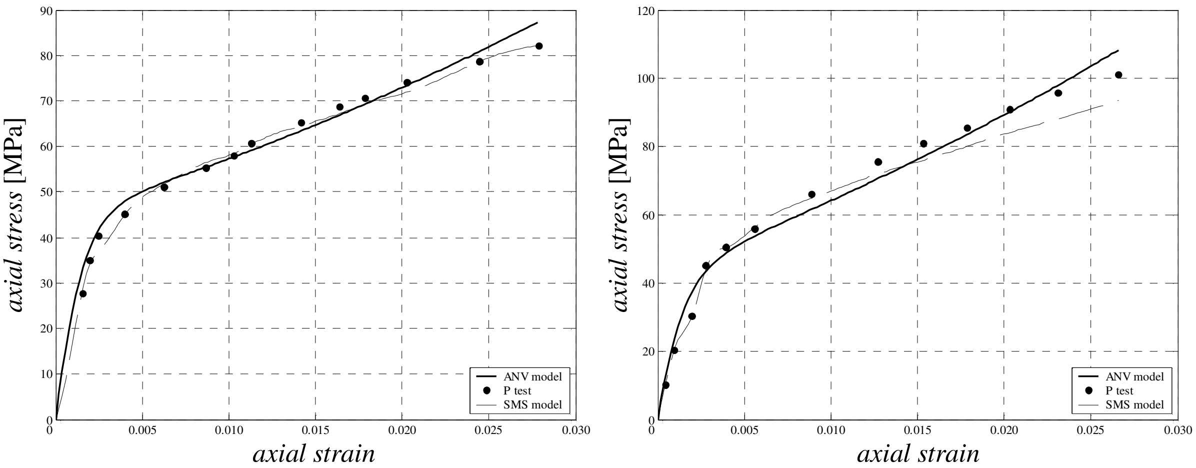

Figure 5. (a) *P.1* test vs. *SMS* and *ANV* models; (b) *P.2* test vs. *SMS* and *ANV* models

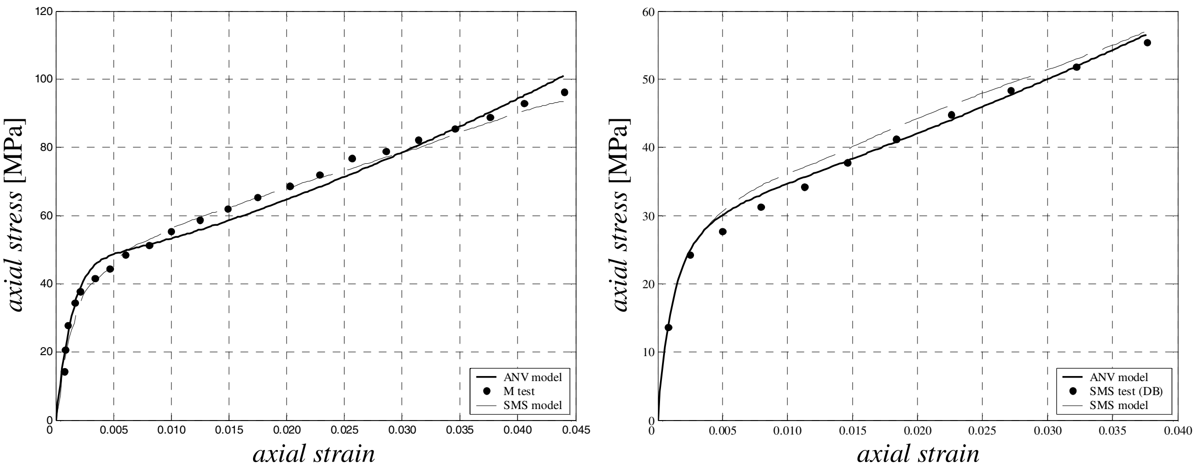

Figure 6. (a) *PRL* test vs. *SM, FR* and *ANV* models; (b) *SMS.1* test vs. *SMS* and *ANV* models

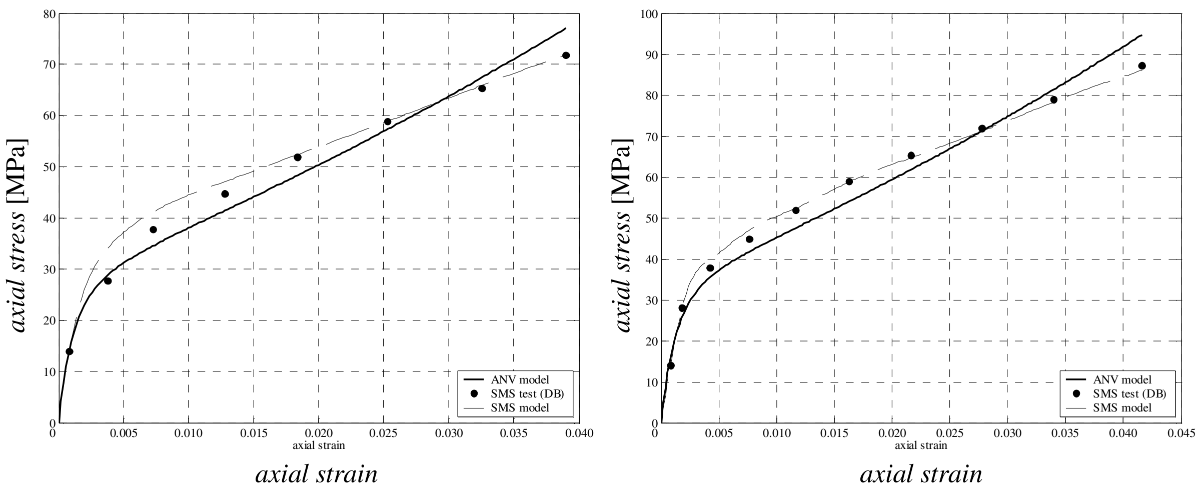

Figure 7. (a) ***SMS.2*** **test vs.** ***SMS*** **and** ***ANV*** **models; (b)** ***SMS.3*** **test vs.** ***SMS*** **and** ***ANV*** **models**

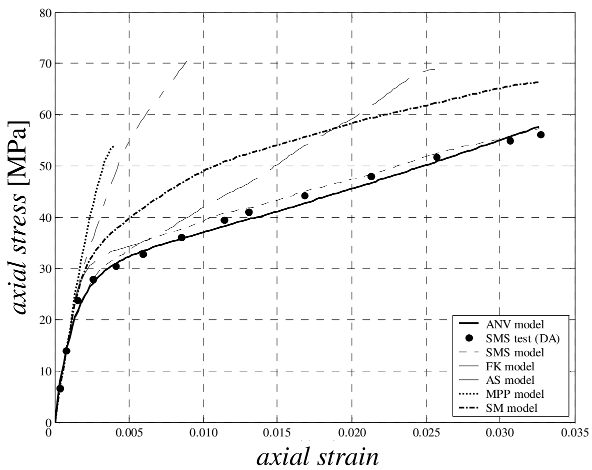

Figure 8. ***SMS.4*** **test vs.** ***SMS***, ***FK***, ***AS***, ***MPP***, ***SM*** **and** ***ANV*** **models**

Ratios between predicted and observed tensions at failure are shown in Table 3. Values of strength are in good agreement.

Table 3. Experimental and Predicted (*ANV* model) Strength for FRP-Confined Concrete Squat Specimens.

Acronym	Experimental strength (MPa)	Predicted strength (MPa)	Ratio between predicted and experimental strength
FR	64.00	66.21	1.034
KHH_1	70.45	67.56	0.959
KHH_2	89.77	97.24	1.083
M	96.19	100.24	1.042
P_1	82.06	86.50	1.054
P_2	100.90	107.36	1.064
PRL	55.97	57.32	1.024
SMS_1	55.33	56.59	1.023
SMS_2	71.80	77.50	1.079
SMS_3	87.10	94.80	1.088
SMS_4	56.03	58.06	1.036

The agreement between the experimental data and the predictions of all the models (*ANV* included) is generally good. A slightly superior performance in precision must be credited to *physically* based models which solve the coupled equilibrium displacement problem in longitudinal and transverse directions at each step of the loading process, e.g. Spoelstra and Monti, and Fam and Rizkalla. However the latter models allow only numerical (not closed form) solutions to the problem, involve programming effort and are computationally not effective. On the other hand, *experimentally* based models, e.g. Saaman, Mirmiran and Shahawy, are easier to understand and program and rather accurate when modeling specimens with simple behaviors, but are intrinsically incapable of detailing complex behaviors in the transition zone between the two main linear trends in the constitutive relationship describing unconfined concrete law and FRP-concrete interaction.

Physical models as the ANV are capable of reproducing cases in which, due to small confinement stiffness ratio k_{fc} the tangent modulus may results negative as shown in the *FR* test, where k_{fc}=0.023. All the other tests considered have k_{fc}, higher than 0.040, and therefore (see Figure 1(b) and Figure 2(a)) the tangent modulus is positive on the entire range of deformation and experimental models result, with the exception of the *FR* test , well capable of reproducing the behavior.

The features of the proposed *ANV* model are somewhat of a compromise between physically and experimental classes. The model is accurate, as can be seen from the experiments-model comparisons, capable of solving the transition zone problem and expressed in closed form. Furthermore, its precision might be improved using a parabolic law for the approximation in Eq. (11) instead of the linear one. However the resulting formulation would be far more complex than for the linear approximation. The latter has been considered the optimal solution for practical applications.

Recall that the *ANV* model should be accurate (errors lower than 7%) up to values of about 0.70 for $\bar{\sigma}_r$ and thereafter its precision should decrease. The value of $\bar{\sigma}_r$ at failure is therefore the key parameter to assess the applicability of this model.

The precision of the *ANV* model is very high with tests having low values of $\bar{\sigma}_r$ at failure (see Table 4) and slightly decreases with increasing values of $\bar{\sigma}_r$. The precision in the lateral tests prediction, *KHH_1*, *KHH_2* and *PRL*, is rather good too.

Table 4. Values of $\bar{\sigma}_r$ at failure for the experiments (n.a.=not available)

Acronym	*FR*	*KHH.1*	*SMS.4*	*SMS.1*	*PRL*	*KHH.2*	*SMS.2*	*M*	*SMS.3*	*P.1*	*P.2*
$\bar{\sigma}_{rfailure}$	0.202	0.244	0.321	0.334	0.371	0.403	0.564	0.634	0.842	n.a.	n.a.

DESIGN CHARTS FOR SQUAT TUBES

Since the constitutive model for squat tubes is expressed in closed form, a design procedure can be set up. The procedure uses the two diagrams in Figure 9 and Figure 10 which respectively show, for a monotonic load process:

- the increase in concrete strength due to confinement;
- the possibility that a softening branch is encountered during the load process.

The increase in concrete strength, Figure 9, is expressed as a function of the confinement stiffness ratio k_{fc} and of the unconfined concrete strength f'_{co}. A couple of values (k_{fc}; f'_{co}) locates a point which lies on one of the curves shown. The value written on each of the curve is the expected increase in strength due to confinement, expressed with respect to the unconfined concrete strength.

For instance, a 25 MPa unconfined strength concrete, when confined with a FRP jacket with k_{fc}=0.025, will have a confined strength equal to $2.2 \cdot f'_{co}$=55 MPa. The values in Figure 9 have been computed via Eqs. (7), (8) and (14) which, after rearrangement, yield:

$$\frac{f'_{cc}}{f'_{co}} \cong 1 + 3.609 \cdot k_{fc} \cdot \frac{\varepsilon_l}{\varepsilon'_{co}} = 1 + 3.609 \cdot \frac{E_{jho}}{f'_{co}} \cdot \frac{t}{R} \cdot \varepsilon_l \tag{26}$$

ε'_{co} has been set equal to 0.002 while for ε_l the value of 0.03 has been chosen. The latter corresponds to the traction failure strain for S-glass reinforced polymers and is about the maximum strain for commercial FRP's (Matthews [4]).

Figure 10 shows, instead, once k_{fc} and f'_{co} have been set, which will be the minimum tangent stiffness on the f_{cc}-ε_{cc} constitutive model during a monotonic load process up to failure. Consider the f_{cc}-ε_{cc} constitutive models as shown in Figure 1(b) and the associated values of the tangent stiffness $df_{cc}/d\varepsilon_{cc}$ shown in Figure 2(a). Once values for ν_{co}, ε'_{co}, f'_{co} and α have been set, the choice of a particular value of k_{fc} singles out one of the curves in Figure 1(b) and one of the curves in Figure 2(a). The minimum of this curve in Figure 2(a) is the minimum tangent stiffness $df_{cc}/d\varepsilon_{cc}$ during a monotonic load process up to failure and this value is then shown in Figure 10, normalized with respect to the initial tangent modulus of unconfined concrete $E_{co} = \alpha\sqrt{f'_{co}}$.

For instance, from Figure 10, one can see that a 30 MPa unconfined strength concrete, during a monotonic load process up to failure, will always show positive tangent stiffness (i.e. no descending branches in the f_{cc}-ε_{cc} constitutive law) for stiffness ratios k_{fc} higher than about 0.038, the reverse being true for k_{fc} lower than 0.038.

As an example of use of the design charts consider the following:

(i) an FRP-concrete tube must be designed to carry a load of 2000 kN. The concrete unconfined strength is equal to 30 MPa and the column diameter is 0.50 m;

(ii) with these data, the average stress carried by concrete is $\sigma_{avg}=N/(\pi R^2)=10$ MPa and the design resistance must be higher than $\sigma_d=\eta_c\cdot\sigma_{avg}$. η_c is a safety factor which is currently given a value of 5. Thus $\sigma_d=50$ MPa and the increase in strength which must be obtained with jacketing is $\sigma_d/f'_{co}=50/30\cong1.67$;

(iii) from Figure 9, for a 30 MPa concrete and a desired increase in strength of 1.67, one reads a value for k_{fc} equal to 0.018;

(iv) from the definition of $k_{fc}=E_{jho}\cdot t/(E_{cs}\cdot R)$, one computes $E_{jho}\cdot t=k_{fc}\cdot E_{cs}\cdot R=0.018\cdot30/0.002\cdot0.25=$ 67.5 MPa·m;

(v) if one uses S-glass FRP, then $E_{jho}\cong60$ GPa and the value of t is equal to 67.5 MPa·m /60 GPa=1.1 mm;

(vi) from Figure 10, finally, one can check what will be the FRP-concrete tube behavior for unexpected increases of load. Since, as already noticed, for a 30 MPa unconfined strength concrete, if $k_{fc}<0.038$ the tangent stiffness may be negative, such will be the behavior of the designed column, in the post peak-strength range.

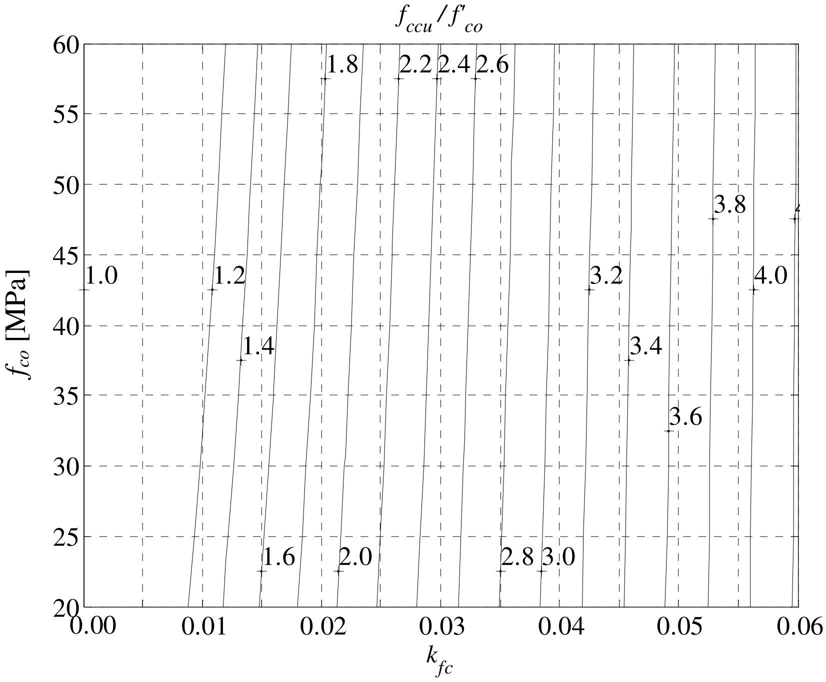

Figure 9. Increase in strength due to confinement (ε'_{co}=0.002, ε_l=0.030 corresponding to S-glass FRP)

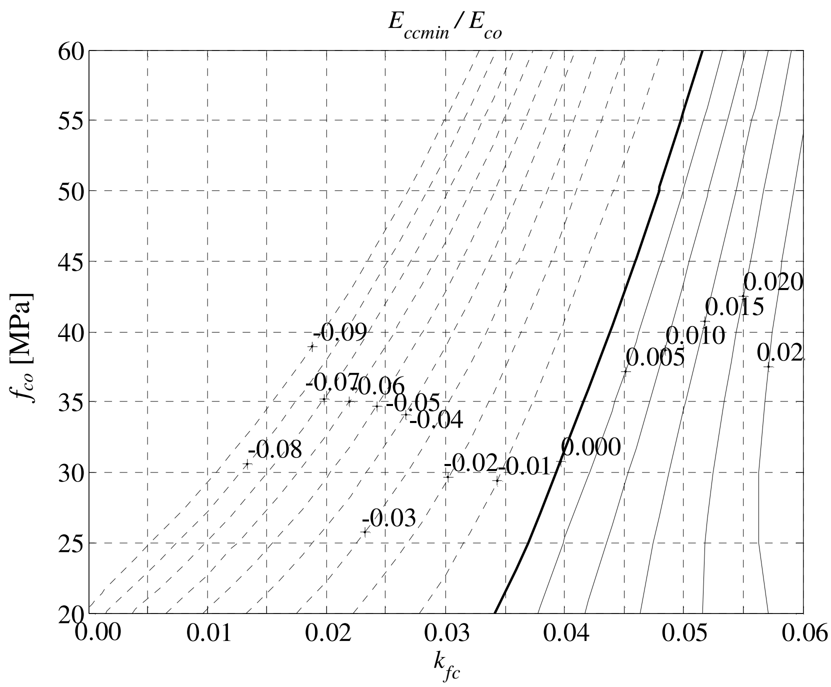

Figure 10. Minimum of tangent stiffness of constitutive model (ν_{co}=0.15; ε'_{co}=0.002; α=5,000)

CONCLUSIONS

In the paper, a model for the longitudinal and transverse behavior of FRP tubes filled with concrete and loaded in compression is presented. The equilibrium/compatibility problem is solved for squat tubes (i.e. buckling is not considered) and then extended to also include instability effect (Albanesi [1]). The most interesting features of the model are its capability to reproduce the details of the constitutive law, e.g. degrading branches followed by positive stiffness branches, while being simple enough and expressed in closed form. The model is suited to be inserted in non linear finite element codes. A design procedure has also been set up and its key results presented in charts.

The model is validated for squat tubes. The agreement with experimental data is, in the authors' opinion, good.

Two remarks must be done on the potential applications for the model. First, the use of this very model is not limited to FRP wrapped concrete cylinders but can be extended to model other types of jacketing, including steel – jackets. Secondly, what has been developed up to now is the monotonic constitutive law which can be used to reproduce static tests. However, among the most interesting applications of the model, the study of seismic retrofitting of columns with FRP wrapping is certainly appealing. This is not possible at the present state of development, because only pure compression and monotonic loads have been considered. However the extension to seismic case can be made regarding the present constitutive law as the skeleton curve.

These aspects, together with the extension to cases in which also a bending moment is present will be the object of further research.

REFERENCES

1. Albanesi, T, Nuti, C, Vanzi, I. "Legame uniassiale tensione-deformazione per calcestruzzo confinato con frp." XI Congresso Nazionale ANIDIS "L'Ingegneria sismica in Italia", Genova, Italy, 2004.
2. Song, YL, Chen, JF. "Structural behaviour of short steel-concrete composite spun tubular columns." Magazine of Concrete Research, 2000; 52(6): 411-418.
3. Park, R, Paulay, T. *Reinforced concrete structures*, John Wiley & Sons, New York, 1975.
4. Matthews, FL, Rawlings, RD. *Composite materials: Engineering and Science*. Chapman and Hall, London, UK, 1996.

5. Lam, L, Teng, JG. "Strength models for fiber-reinforced plastic-confined concrete." *J. of Struct. Engrg.*, ASCE, 2002; 128(5): 612-623.
6. Teng, JG, Chen, JF, Smith, ST, Lam, L. "FRP strengthened RC structures." John Wiley & Sons, Chichester, UK, 2002.
7. Spoelstra, M R, Monti, G. "FRP-confined concrete model." *J. of Composite Material in Constructions*. ASCE, 1999; 3(3): 143-150.
8. Fam, AZ, and Rizkalla, SH. "Confinement model for axially loaded concrete confined by circular fiber-reinforced polymer tubes." *ACI Struct. J.*, 2001; 98(4): 451-461.
9. Pantazopolou, SJ, Mills, RH. "Microstructural aspects of the mechanical response of plain concrete." *ACI Mat. J.*, 1995; 92(Nov.-Dec.): 605-616.
10. Mander, JB, Priestley, MJN, Park, R. "Theoretical stress-strain model for confined concrete." *J. of Struct. Engrg.*, ASCE, 1988; 114(8): 1804-1826.
11. Samaan, M, Mirmiran, A, Shahawy, M. "Model of concrete confined by fiber composite." *J. of Struct. Engrg.*, ASCE, 1998; 124(9): 1025-1031.
12. Gardner, NJ. "Triaxial behavior of concrete." *ACI J. Proc.*, 1969; 66(2): 136-146.
13. Hollaway, LC, Head, PR. "Advanced polymer composites and polymers in the civil infrastructure." Elsevier, Amsterdam, 2001.
14. Mirmiran, A. "Hybrid fiber reinforced polymer (FRP)-concrete column." *Final Report*, *Contract No. BA-519*, Florida Dept. of Transportation, Tallahassee, University of Central Florida, Florida, 1999.
15. Kawashima, K, Hosotani, M, Hoshikuma, J. "A model confinement effect for concrete cylinders confined by carbon fiber sheets." *NCEER-INCEDE Workshop on Earthquake Engineering Frontiers in Transportation Facilities*, NCEER, State University of New York, Buffalo, N.Y., 1997.
16. Picher, F. "Confinement de cylinders en béton par des composites carbone-époxy unidirectionnels." MS thesis, University of Sherbrooke, Sherbrooke, Canada (in French), 1995.
17. Picher, F, Rochette, P, Labossiere, P. "Confinement of concrete cylinders with CFRP." *Proc., 1st International Conference on Composites in Infrastructure*, H. Saadatmanesh and M. R. Ehsani, eds., University of Arizona, Tucson, Ariz.: 829-841, 1996.
18. Ahmad, SH, Shah, SP. "Stress-strain curves of concrete confined by spiral reinforcement." *ACI Struct. J.*, 1982; 79(6): 484-490.
19. Fardis, MN, Khalili, HH. "FRP-encased concrete as a structural material." *Mag. Of Concrete Res.*, 1982; 34(121): 191-201.
20. Knowles, RB, Park, R. "Strength of concrete filled steel tubular columns." *Journal of the Structural Division*, Proceedings of the American Society of Civil Engineers, ST12: 2565-2587, 1969.